Influence of the elemental composition of the metal phase of the Co-MgF_2 and CoFeZr-MgF_2 composites on the magnetotransport properties

© T.V. Tregubova, O.V. Stognei, I.M. Tregubov

Voronezh State Technical University,
Voronezh, Russia

E-mail: ttv1507@ya.ru

Received May 12, 2023
Revised September 14, 2023
Accepted October 30, 2023

The physical properties and structure of nanogranular thin-film composites $Co_x(MgF_2)_{100-x}$ and $(Co_{47}Fe_{42}Zr_{11})_x(MgF_2)_{100-x}$ are studied in a wide range of concentrations of the metal phase ($14 \le x$, at.% ≤ 62 and $15 \le x$, at.% ≤ 55). The systems were studied in the initial state and after heat treatment at various temperatures in a vacuum atmosphere up to 350°C. The systems under study exhibit magnetoresistive properties. The maximum values of negative magnetoresistance (MR) reach 7% and 3.25%, respectively. $Co_x(MgF_2)_{100-x}$ composites, in contrast to $(CoFeZr)_x(MgF_2)_{100-x}$ composites, exhibit positive tunneling magnetoresistance.

Keywords: nanogranular composites, magnetoresistance, anisotropy, thermal stability.

DOI: 10.61011/PSS.2023.12.57666.5144k

Samples of composites $Co_x(MgF_2)_{100-x}$ and $(Co_{47}Fe_{42}Zr_{11})_x(MgF_2)_{100-x}$ were obtained by ion-beam sputtering of composite targets. The thickness of the resulting films varies from 1 to 3 μm depending on the metal phase concentration. The elemental composition of the composites was monitored using electron probe X-ray microanalysis (JXA-840). The structure was studied using X-ray diffraction analysis (BRUKER D2 Phaser). To study the electrical and magnetoresistive properties of composite samples, a two-probe potentiometric method was used. The magnetoresistance of the samples was studied in two geometries. The main measurements were carried out with parallel orientation of the electric current flowing through the sample and the external magnetic field. To confirm the isotropy of the magnetoresistive effect, additional measurements were carried out in which the current was oriented perpendicular to the field. The magnetic properties of the composites were studied using a vibrating magnetometer. The magnetic and magnetoresistive properties were studied sing the same magnetizing system, which ensured the adequacy of the comparison of the obtained characteristics. All measurements were performed at room temperature.

The composites obtained for study differ in the composition of the metal phase: in the first composite system, the metal phase is formed from pure cobalt, in the second — the metal phase is formed from the alloy $Co_{47}Fe_{42}Zr_{11}$. Zirconium in this alloy is an amorphizing element; therefore, when this material is sputtered, the structure of the films formed is, as a rule, amorphous [1–3]. However, in sputtered composites $(Co_{47}Fe_{42}Zr_{11})_x(MgF_2)_{100-x}$ X-ray diffraction analysis showed that the metal phase is crystalline, and the structure of this phase corresponds to CoFe alloy with a cubic structure (space group Pm3m, $a = 2.8552$Å). Moreover, the angular position of the diffraction peaks practically corresponds to the tabulated values; only a slight shift of 2Θ to the region of large angles by 0.1–0.3 degrees is observed. This indicates that in the metal phase there is no increase in the lattice constant, which should be observed in the case of „dissolution“ of 11 at.% zirconium. The dielectric phase of B composites $(Co_{47}Fe_{42}Zr_{11})_x(MgF_2)_{100-x}$ also has a crystalline structure, and the presence of two modifications was established. Tetragonal MgF_2 (P42/mnm, $a = 4.69$ Å, $c = 3.096$ Å) which is the equilibrium phase and tetragonal MgF_2 with a modified lattice (P4/nmm, $a = 4.06$ Å, $c = 3.82$ Å). The results obtained suggest that during the composite structure the formation (which occurs as a result of self-organization of condensing atoms), zirconium atoms dissolve in magnesium fluoride. In this case, the metal alloy, depleted in the amorphizer, crystallizes, and magnesium fluoride forms two modifications, one of which, MgF_2 (P4/nmm), is metastable and is stabilized by dissolved zirconium. This modification disappears after vacuum annealing of the composites at 350°C [4], while the first fluoride modification (P42/mnm, $a = 4.69$ Å, $c = 3.096$ Å) — is preserved.

Composites $Co_x(MgF_2)_{100-x}$ are also crystalline: metal phase — hexagonal cobalt, dielectric phase — tetragonal magnesium fluoride (P42/mnm, $a = 4.69$ Å, $c = 3.096$ Å). Thus, both systems studied, despite the difference in the elemental composition of the metal phases, are completely crystalline.

The study of the electrical properties of the resulting nanocomposites showed that the concentration position of the electrical percolation threshold is significantly shifted to the region with a lower content of the metal phase compared to composites formed on the basis of oxide dielectrics, see Table [5,6–8]. The position of the percolation threshold

Position of the percolation threshold in metal-dielectric composites

Composite composition	Position of percolation threshold, at.% Me	Composite composition	Position of percolation threshold, at.% Me
$Co_x(MgF_2)_{100-x}$	35	$Co_x(SiO_2)_{100-x}$ $Co_x(Al_2O_3)_{100-x}$	52 64
$(Co_{47}Fe_{42}Zr_{11})_x(MgF_2)_{100-x}$	27	$(Co_{45}Fe_{45}Zr_{10})_x(SiO_n)_{100-x}$ $(Co_{45}Fe_{45}Zr_{10})_x(Al_2O_n)_{100-x}$	40 50
		$(Co_{41}Fe_{39}B_{20})_x(SiO_n)_{100-x}$ $(Co_{86}Nb_{12}Ta_2)_x(Al_2O_n)_{100-x}$	50 44

in all the above systems was determined using the same method [5]. Apparently, the shift in the percolation threshold is due to the higher chemical activity of magnesium compared to the elements that form the oxide phases of the composites (silicon or aluminum).

Regardless of the metal phase composition, prepercolation composites are characterized by the presence of negative tunneling magnetoresistance (MR). Maximum MR values were found near the percolation threshold both in composites $Co_x(MgF_2)_{100-x}$ and in composites $(Co_{47}Fe_{42}Zr_{11})_x(MgF_2)_{100-x}$ [7]. However, the absolute values of the MR of composites of different systems differ by almost two times. The maximum value of MR, reaching 7%, is observed in composites $Co_x(MgF_2)_{100-x}$ at the same time in composites $(Co_{47}Fe_{42}Zr_{11})_x(MgF_2)_{100-x}$ the maximum MR is 325%. It is characteristic that the maximum value of magnetoresistance obtained in the system $(Co_{47}Fe_{42}Zr_{11})_x(MgF_2)_{100-x}$, composites is close in value to the maximum value obtained with an oxygen matrix $(Co_{45}Fe_{45}Zr_{10})_x(SiO_2)_{100-x} = 3.8\%$ [8], and MS value of composites $Co_x(MgF_2)_{100-x}$ is comparable with magnetoresistance of com[posites $Co_x(Al_2O_3)_{100-x}$ (6.5%) [9]. This confirms the thesis that the magnitude of the magnetoresistive effect is largely determined by the composition of the metal phase [5].

The magnetoresistive effect observed in nanocomposites $Co_x(MgF_2)_{100-x}$, differs from such in nanocomposites $(Co_{47}Fe_{42}Zr_{11})_x(MgF_2)_{100-x}$ by not only value, but in that in samples $Co_x(MgF_2)_{100-x}$ in addition to the usual negative magnetoresistance, isotropic positive magnetoresistance (PMR) is also observed (Figure 1, *a*). The PMR isotropy is manifested in that the magnitude and shape of the field dependence of the magnetoresistance of composites does not depend on the mutual orientation of the electric current and magnetic field. The shape of the curves is the same for both parallel and perpendicular orientations of the field and current. This proves the tunnel nature of PMR. PMR is observed only in samples located at the percolation threshold (31–38 at.% Co), i. e., in samples with a complex morphology containing not only individual granules, but also percolation clusters beginning to form [5]. At the same time, it is obvious that the same morphology also exists in composites $(Co_{47}Fe_{42}Zr_{11})_x(MgF_2)_{100-x}$, located at the percolation threshold, however, no PMR is observed there (Figure 1, *b*). It is important to note that previously positive tunneling magnetoresistance was observed in prepercolation composites with a cobalt metal phase but with an oxide matrix: Co-Al_2O_3 and Co-SiO_2 [9–11]. It follows that the appearance of PMR is associated with the features of the physical properties of the nanoscale cobalt phase. Apparently, this is due to the high magnetic anisotropy of cobalt, which has a hexagonal structure. Magnetic anisotropy is

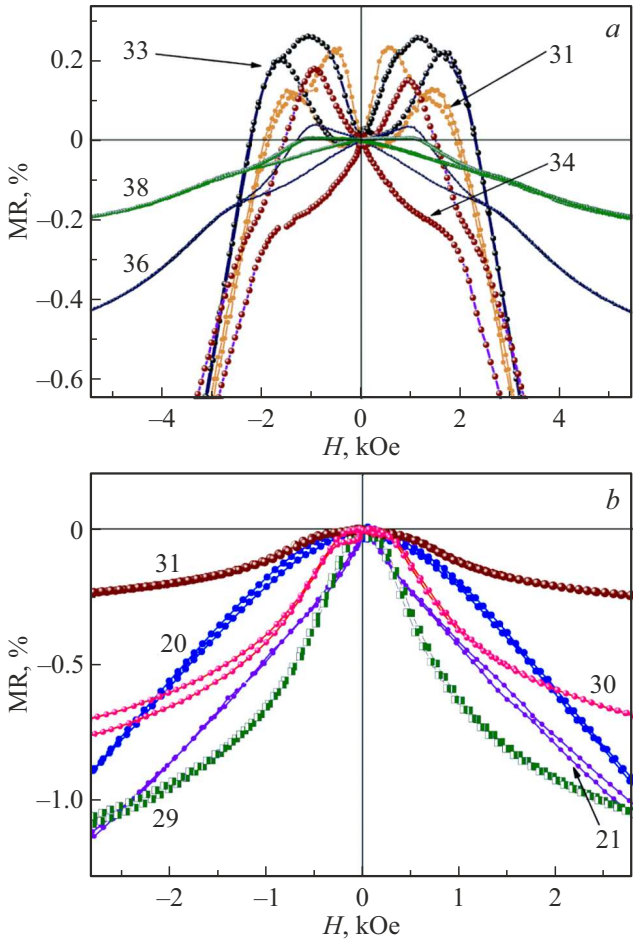

Figure 1. Field dependences of magnetoresistance of com[posites $Co_x(MgF_2)_{100-x}$ (*a*) and $(CoFeZr)_x(MgF_2)_{100-x}$ (*b*) with different concentrations of the metal phase. The concentration of the metal phase (at.%) is shown in the graphs.

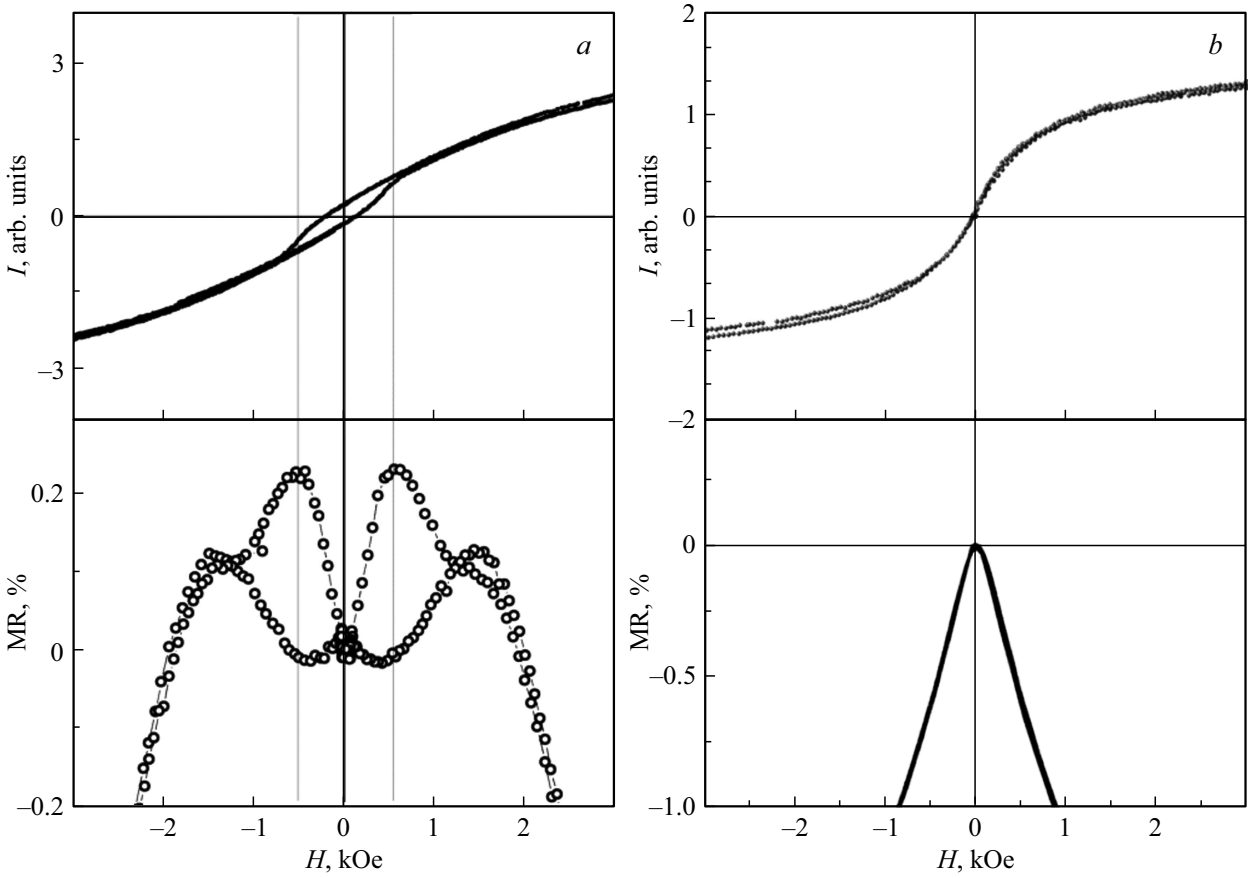

Figure 2. Magnetization and magnetoresistance vs. magnetic field strength for the composite $Co_{32}(MgF_2)_{68}$ (a) and $(CoFeZr)_{26}(MgF_2)_{74}$ (b).

important for the processes of reorientation of the magnetic moments of granules and clusters by an external field and largely determines the field dependences of the resistance of composite materials [5,9,11]. Comparison of magnetic anisotropy constants for HCP Co ($K_1 = 6.81 \cdot 10^5$, $K_2 = 1.75 \cdot 10^5$ kJ/m^3 [12]) and crystalline alloy $Co_{50}Fe_{50}$ ($K_1 = -6.8 \cdot 10^{-1}$, $K_2 = -3.90$ kJ/m^3 [13]) shows that the difference in values exceeds five orders of magnitude. This means that in weak magnetic fields, composites $Co_x(MgF_2)_{100-x}$, which are at the percolation threshold and have a complex morphology (the simultaneous presence in the structure of the composite of both nanograins and relatively large clusters), remagnetize other than composites $(Co_{47}Fe_{42}Zr_{11})_x(MgF_2)_{100-x}$ with a similar complex morphology. In composites with a metal phase from alloy CoFe with low anisotropy, simultaneous remagnetization of both granules and clusters occurs, while in composites with highly anisotropic metal phase of cobalt, granules are first remagnetized and only then clusters, in which the anisotropy is higher, begin to remagnetize due to their larger size. Thus, in composites with cobalt metal phase in weak magnetic fields the maximum misorientation of magnetic moments is realized (the granules are already remagnetized, but the clusters are not yet) [9], which leads to a maximum resistance not in zero field, as it occurs in composites $(Co_{47}Fe_{42}Zr_{11})_x(MgF_2)_{100-x}$, and in some non-zero field in Figure 1, a.

The fact that the processes of reorientation of the magnetic moments of granules and clusters in $Co_x(MgF_2)_{100-x}$ composites are influenced by anisotropy is confirmed by the appearance of the remagnetization curves. Figure 2, a shows the field dependences of magnetization and magnetoresistance of the composite $Co_{32}(MgF_2)_{68}$, located at the percolation threshold. The magnitude of the MR in this sample in field of 9 kOe is 2.5%, however, magnetic hysteresis is obviously present on the magnetization curve. Usually, the presence of magnetic hysteresis in composite samples means that the sample composition is „beyond" the percolation threshold, macroscopic domains are formed in it, and from a magnetic point of view it is no longer a superparamagnetic, but a ferromagnetic [5,10]. In such composites, the magnetoresistive effect is not observed because the physical reason for its occurrence disappears: the magnetic moments of neighboring granules are oriented parallel to each other, regardless of the presence or absence of magnetic field, therefore the magnitude of the tunnel current is the same in the field and without the field. However, in our case (Figure 2, a) both MR and magnetic

hysteresis are present. This is due to the fact that the cause of hysteresis is not the domain walls pinning, but the magnetic anisotropy of nanoscale cobalt clusters. Moreover, the value of the anisotropy field, determined from the remagnetization curve, exactly coincides with the field corresponding to the maximum magnetoresistance. In other words, in a field in which the magnetic hysteresis „closes", the remagnetization of clusters begins, and this means that the system of magnetic moments of granules and clusters begins to become more collinear. This leads to increase in the probability of electron tunneling between granules and clusters and, accordingly, to decrease in electrical resistance, which is observed in the experiment (Figure 2, *a*). It is characteristic that in the composite $(Co_{47}Fe_{42}Zr_{11})_{26}(MgF_2)_{74}$, located at the percolation threshold and having a complex morphology, there is no PMR and magnetic hysteresis (Figure 2, *b*). The reason for this is the low value of magnetic anisotropy of the metal phase, which causes simultaneous remagnetization of both granules and clusters.

Thus, the elemental composition of the metal phase of the composites $Co_x(MgF_2)_{100-x}$ and $(Co_{47}Fe_{42}Zr_{11})_x(MgF_2)_{100-x}$ determines the nature of their magnetotransport properties near the percolation threshold. In composites $Co_x(MgF_2)_{100-x}$, the presence of large crystallographic anisotropy in cobalt nanograins leads to the appearance of positive magnetoresistive effect, as well as to the simultaneous occurrence of magnetic hysteresis and magnetoresistive effect, which is not typical for composites. In composites $(Co_{47}Fe_{42}Zr_{11})_x(MgF_2)_{100-x}$ with low anisotropy of the metal phase (CoFe), magnetic and magnetoresistive properties are typical for metal-dielectric composites.

Funding

The paper was supported by the Ministry of Science and Higher Education of the Russian Federation within the framework of the state order No. 2023-0006).

Conflict of interest

The authors declare that they have no conflict of interest.

References

[1] J.A. Fedotova, A. Saad, A. Larkin, V. Fedotova, Y. Ilyashuk, A. Fedotov, Y. Kalinin, A. Sitnikov. In: 9th IEEE Conf. on Nanotech. Genoa, Italy (2009). P. 651.
[2] J.-O. Song, S.-R. Lee. JMMM **310** (2007). DOI: 10.1016/j.jmmm.2006.10.608
[3] J.A. Fedotova, A.V. Pashkevicha. JMMM **511** 166963 (2020). DOI: 10.1016/j.jmmm.2020.166963
[4] O.V. Stognei, T.V. Tregubova, I.M. Tregubov. Lett. Mater. **13**, *2*, 109 (2023). DOI: https://doi.org/10.22226/2410-3535-2023-2-109-114
[5] S.A. Gridnev, Yu.E. Kalinin, A.V. Sitnikov, O.V. Stogney. Nelinejnye yavleniya v nano- i mikrogeterogennykh sistemakh. BINOM. Laboratoriya znanij, M. (2012). P. 136–138. (in Russian),
[6] I.A. Svito, A.K. Fedotov, A. Saad, P. Zukowski, T.N. Koltunowicz. J. Alloys. Comp. **699**, 818 (2017). DOI: https://doi:10.1016/j.jallcom.2017.01.043
[7] T.V. Tregubova, O.V. Stognei, V.V. Kirpan, A.V. Sitnikov. In: *EPJ Web of Conf. MISM* **185**, 01014 (2018). DOI: org/10.1051/epjconf/201818501014
[8] O.V. Stognei, V.A. Slyusarev. Microelectron. Eng. **69**, *2–4*, 476 (2003). DOI: 10.1016/s0167-9317(03)00359-9
[9] A. Granovsky, Y. Kalinin, A. Sitnikov, O. Stognei. Phys. Procedia **82**, 45 (2016). DOI: https://doi: 10.1016/j.phpro.2016.05.009
[10] O.V. Stogney, A.V. Sitnikov, Yu.E. Kalinin, S.F. Avdeev, M.N. Kopytin. FTT **49**, *1*, 158 (2007). (in Russian).
[11] A.A. Timofeev, S.M. Ryabchenko, A.F. Lozenko, P.A. Trotsenko, O.V. Stogneĭ, A.V. Sitnikov, S.F. Avdeev. Low Temp. Phys. **33**, *11*, 974 (2007). DOI: https://doi.org/10.1063/1.2747075
[12] S.F. Avdeev, V.V. Strelnikova, A.V. Sitnikov. Vestn. Voronezh. gos. tekh. un-ta, **33**, *11*, 1282 (2007). (in Russian).
[13] W.R. Angus, J. Favéde, J. Hoaru, A. Pacault, John H. Van Vleck. Phys. Today **22**, *7*, 86 (1969). DOI: https://doi.org/10.1063/1.3035705

Translated by I.Mazurov